Development and characterization of anti-glycopeptide monoclonal antibodies against human podoplanin using glycan-deficient cell lines generated by CRISPR/Cas and TALEN

Mika K. Kaneko[1], Takuro Nakamura[1], Ryusuke Honma[1,2], Satoshi Ogasawara[1], Yuki Fujii[1], Shinji Abe[3,4], Michiaki Takagi[2], Hiroyuki Harada[5], Hiroyoshi Suzuki[6], Yasuhiko Nishioka[4], Yukinari Kato[1]

[1]Department of Regional Innovation, Tohoku University Graduate School of Medicine, 2-1 Seiryo-machi, Aoba-ku, Sendai, Miyagi 980-8575, Japan

[2]Department of Orthopaedic Surgery, Yamagata University Faculty of Medicine, 2-2-2 Iida-nishi, Yamagata 990-9585, Japan

[3]Department of Clinical Pharmacy Practice Pedagogy, Institute of Biomedical Sciences, Tokushima University Graduate School, 1-78-1 Sho-machi, Tokushima 770-8505, Japan

[4]Department of Respiratory Medicine and Rheumatology, Institute of Biomedical Sciences, Tokushima University Graduate School, 3-18-15 Kuramoto-cho, Tokushima 770-8503, Japan

[5]Oral and Maxillofacial Surgery, Graduate School of Medical and Dental Sciences, Tokyo Medical and Dental University, 1-5-45, Yushima, Bunkyo-ku, Tokyo 113-8510, Japan

[6]Department of Pathology and Laboratory Medicine, Sendai Medical Center, 2-8-8, Miyagino, Miyagino-ku, Sendai, Miyagi 983-0045, Japan

Corresponding author: Yukinari Kato

Tohoku University Graduate School of Medicine, 2-1 Seiryo-machi, Aoba-ku, Sendai,

Miyagi 980-8575, Japan; E-mail: yukinari-k@bea.hi-ho.ne.jp; or, yukinarikato@med.tohoku.ac.jp; TEL/FAX: +81-22-717-8207

Abstract

Human podoplanin (hPDPN), which binds to C-type lectin-like receptor-2 (CLEC-2), is involved in platelet aggregation and cancer metastasis. The expression of hPDPN in cancer cells or cancer-associated fibroblasts indicates poor prognosis. Human lymphatic endothelial cells, lung type I alveolar cells, and renal glomerular epithelial cells express hPDPN. Although numerous monoclonal antibodies (mAbs) against hPDPN are available, they recognize peptide epitopes of hPDPN. Here, we generated a novel anti-hPDPN mAb, LpMab-21. To characterize the hPDPN epitope recognized by the LpMab-21, we established glycan-deficient CHO-S and HEK-293T cell lines using the CRISPR/Cas9 or TALEN. Flow cytometric analysis revealed that the minimum hPDPN epitope, in which sialic acid is linked to Thr76, recognized by LpMab-21 is Thr76–Arg79. LpMab-21 detected hPDPN expression in glioblastoma, oral squamous carcinoma, and seminoma cells as well as in normal lymphatic endothelial cells. However, LpMab-21 did not react with renal glomerular epithelial cells or lung type I alveolar cells, indicating that sialylation of hPDPN Thr76 is cell-type specific. LpMab-21 combined with other anti-hPDPN antibodies that recognize different epitopes may therefore be useful for determining the physiological function of sialylated hPDPN.

Key words: podoplanin, monoclonal antibody, glycopeptide, epitope, sialic acid

Abbreviation: PDPN, podoplanin; hPDPN, human podoplanin; CLEC-2, C-type lectin-like receptor-2; mAbs, monoclonal antibodies; CHO, Chinese hamster ovary; CRISPR, clustered regularly interspaced short palindromic repeat; TALEN, transcription activator-like effector nuclease; Thr, threonine; Arg, arginine; Glu, glutamic acid; Asp, aspartic

52 acid; PLAG, platelet aggregation-inducing; GpMab, anti-glycopeptide monoclonal
53 antibody; ATCC, American Type Culture Collection; JCRB*;* Japanese Collection of
54 Research Bioresources; LEC, lymphatic endothelial cells; DMEM, Dulbecco's Modified
55 Eagle's Medium; FBS, fetal bovine serum; KO, knockout; L-PHA, leukoagglutinin from
56 *Phaseolus vulgaris*; MAL-II*, Maackia amrensis* Lectin II; i.p., intraperitoneal; ELISA,
57 enzyme-linked immunosorbent assay; BSA, bovine serum albumin; PBS, phosphate-
58 buffered saline; DAB, 3, 3-diaminobenzidine tetrahydrochloride; Ser, serine; PA,
59 podoplanin/aggrus; ADCC, antibody-dependent cellular cytotoxicity; CDC,
60 complement-dependent cytotoxicity
61

62 **Introduction**

63 Human podoplanin (hPDPN) is expressed in many cancers, including
64 malignant gliomas, lung cancers, esophageal cancers, malignant mesotheliomas,
65 testicular cancers, bladder cancers, and osteosarcomas [1-13], and the expression of
66 hPDPN in cancer-associated fibroblasts contributes to poor prognosis [14-19]. Human
67 PDPN (known as the platelet aggregation-inducing factor Aggrus) is involved in cancer
68 metastasis [11, 20, 21]. We identified C-type lectin-like receptor-2 (CLEC-2) as an
69 endogenous receptor of hPDPN [22, 23]. Moreover, our comparative crystallographic
70 studies of the hPDPN–CLEC-2 complex [24] revealed that CLEC-2 binds to hPDPN
71 through residues Glu47 and Asp48 within its platelet aggregation-inducing (PLAG)
72 PLAG3 domain as well as to the α2-6-linked sialic acid linked to Thr52.

73 Analyses using highly sensitive and specific anti-hPDPN mAbs are required to clarify
74 the physiological function of hPDPN in normal tissues and cancers. Although many anti-
75 hPDPN mAbs are available, most react with the hPDPN domains PLAG1-PLAG3 [6, 25-
76 29]. We previously established the original technology to produce anti-glycopeptide
77 mAbs (GpMabs) against hPDPN [30-39]. Here, we generated a novel anti-hPDPN mAb
78 designated LpMab-21 that recognizes a sialylated glycopeptide epitope.

79 Furthermore, to characterize the hPDPN epitope recognized by the LpMab-21, we
80 need glycan-deficient CHO-S or HEK-293T cell lines. We report the establishment of
81 glycan-deficient cell lines using the CRISPR/Cas9 or TALEN.

82

83 **Materials and Methods**

84 **Cell lines, mice, and human tissues**

85 As described in detail previously [36, 39], the cell lines LN229, HEK-293T, NCI-H226,
86 U-2 OS, Met-5A, Chinese hamster ovary (CHO)-K1, and P3U1 were obtained from the
87 American Type Culture Collection (ATCC, Manassas, VA, USA). The HSC-2 and HSC-
88 4 cell lines were obtained from the Japanese Collection of Research Bioresources *(*JCRB*)*
89 Cell Bank (Osaka, Japan). The MG-63 cell line was obtained from the Cell Resource
90 Center for Biomedical Research Institute of Development, Aging and Cancer Tohoku
91 University (Miyagi, Japan). The LN319 cell line was provided by Prof. Kazuhiko
92 Mishima (Saitama Medical University, Saitama, Japan) [40]. Human lymphatic
93 endothelial cells (LECs), CHO-S cells, and PC-10 cells were purchased from Cambrex
94 (Walkersville, MD, USA), Thermo Fisher Scientific Inc., (Waltham, MA, USA), and
95 Immuno-Biological Laboratories Co., Ltd. (Gunma, Japan), respectively. LN229 and
96 CHO-K1 cells were transfected with the hPDPN plasmids using Lipofectamine 2000
97 (Thermo Fisher Scientific Inc.) according to the manufacturer's instructions [30].

98 As described in detail previously [36, 39], CHO-K1, CHO-K1/hPDPN, CHO-S, NCI-
99 H226, PC-10, and P3U1 cells were cultured in RPMI 1640 medium containing L-
100 glutamine (Nacalai Tesque, Inc., Kyoto, Japan). LN229, LN229/hPDPN, LN319, HSC-2,
101 HSC-4, and HEK-293T cells were cultured at 37°C in a humidified atmosphere
102 containing 5% CO_2 in Dulbecco's Modified Eagle's Medium (DMEM) medium
103 containing L-glutamine (Nacalai Tesque, Inc.) and 10% heat-inactivated fetal bovine
104 serum (FBS) (Thermo Fisher Scientific Inc.). LECs were cultured in endothelial cell
105 medium EGM-2MV supplemented with 5% FBS (Cambrex Corp.). All media contained
106 100 units/ml of penicillin, 100 μg/ml of streptomycin, and 25 μg/ml of amphotericin B

107 (Nacalai Tesque, Inc.).

108 As described in detail previously [36, 39], three female BALB/c mice (4-week-old)
109 were purchased from CLEA Japan (Tokyo, Japan) and were housed under pathogen-free
110 conditions. The Animal Care and Use Committee of Tohoku University approved the
111 animal experiments described herein.

112 The Tokyo Medical and Dental University Institutional Review Board and the Sendai
113 Medical Center Review Board reviewed and approved the use of human cancer tissues.
114 Written informed consent was obtained for using the human cancer tissue samples.
115 Microarrays of normal human tissues were purchased from Cybrdi, Inc. (Frederick, MD,
116 USA).

117

118 **Production of glycan-deficient or PDPN-knock out cell lines**

119 The HEK-293T/hPDPN-knockout (KO) cell line (PDIS-2) and the LN319/hPDPN-KO
120 cell line (PDIS-6) were generated by transfection using CRISPR/Cas plasmids (Target
121 ID: HS0000333287) that target PDPN (Sigma-Aldrich, St. Louis, MO). Plasmids were
122 transfected using a Gene Pulser Xcell electroporation system (Bio-Rad Laboratories Inc.,
123 Berkeley, CA, USA) [31, 34]. PDIS-2 and PDIS-6 cells were screened using the NZ-1
124 mAb [5]. The cell lines CHO-S/GnT-1-KO (PDIS-9) and CHO-S/SLC35A1-KO (PDIS-
125 14) were generated by transfecting TALEN or CRISPR/Cas plasmids, which target
126 hsMgat1 (Wako Pure Chemical Industries Ltd., Osaka, Japan) and SLC35A1 (Target ID:
127 HS0000168432; Sigma-Aldrich), respectively, using a Gene Pulser Xcell electroporation
128 system. The cell lines HEK-293T/GnT-1-KO (PDIS-1 or PDIS-12) and HEK-
129 293T/SLC35A1-KO (PDIS-22) were generated by transfecting TALEN or CRISPR/Cas
130 plasmids, which target hsMgat1 (Wako Pure Chemical Industries Ltd., Osaka, Japan) and

131 SLC35A1 (Target ID: HS0000168432; Sigma-Aldrich), respectively, using a Gene Pulser
132 Xcell electroporation system. PDIS-1, PDIS-9, and PDIS-12 cells were screened using
133 leukoagglutinin from *Phaseolus vulgaris* (L-PHA). PDIS-14 and PDIS-22 cells were
134 screened using *Maackia amrensis* Lectin II (MAL-II). PDIS-9 and PDIS-14 cells were
135 transfected with the human PDPN plasmids using Lipofectamine LTX (Thermo Fisher
136 Scientific Inc.) according to the manufacturer's instructions. Glycan-deficient cell lines
137 were cultured in RPMI 1640 medium.
138

139 **Generation of deletion mutants**

140 Amplified hPDPN cDNA was subcloned into a pCAG-Ble(Zeo) vector (Wako Pure
141 Chemical Industries Ltd.) with a MAP-tag, detected by PMab-1 [41, 42], which was
142 added to the N-terminus using the In-Fusion HD Cloning Kit (Clontech, Palo Alto, CA,
143 USA). Deletion mutants of hPDPN were generated using the primers as follows:
144 Sense primers and designation of the corresponding mutant.
145 5′-AGAAGACAAAAAGCTTGCCAGCACAGGCCAGCC, dN23
146 5′-AGAAGACAAAAAGCTTGAAGGCGGCGTTGCCAT, dN37
147 5′-AGAAGACAAAAAGCTTGCCGAAGATGATGTGGTG, dN46
148 5′-AGAAGACAAAAAGCTTACCAGCGAAGACCGCTA, dN55
149 5′-AGAAGACAAAAAGCTTACAACTCTGGTGGCAACA, dN64
150 5′-AGAAGACAAAAAGCTTGTAACAGGCATTCGCATC, dN75
151 5′-AGAAGACAAAAAGCTTACTTCAGAAAGCACAGTCC, N85
152 5′-AGAAGACAAAAAGCTTCAAAGTCCAAGCGCCAC, dN95
153 5′-AGAAGACAAAAAGCTTGCCACCAGTCACTCCAC, dN105
154 Antisense primer

155 5′-TCTAGAGTCGCGGCCGCTTACTTGTCGTCATCGT

156 CHO-K1 cells were transfected with these plasmids using Lipofectamine LTX
157 (Thermo Fisher Scientific Inc.). Deletion mutants were cultured in RPMI 1640 medium
158 containing L-glutamine (Nacalai Tesque, Inc.) and 10% heat-inactivated FBS at 37°C in
159 a humidified atmosphere containing 5% CO_2. Stable transfectants of CHO-K1/ssMAP-
160 hPDPNdN mutants were selected by culturing them in medium containing 0.5 mg/ml
161 Zeocin (InvivoGen, San Diego, CA, USA).

162

163 **Production of point mutants**

164 As described in detail previously [36, 39], the amplified hPDPN cDNA was subcloned
165 into a pcDNA3 vector (Thermo Fisher Scientific Inc.), and a FLAG epitope tag was added
166 to the C-terminus. Substitutions of amino acid residues to Ala or Gly in the hPDPN
167 sequence were performed using a QuikChange Lightning site-directed mutagenesis kit
168 (Agilent Technologies Inc., Santa Clara, CA, USA) using oligonucleotides containing the
169 desired mutations. CHO-S or CHO-K1 cells were transfected with the plasmids using a
170 Gene Pulser Xcell electroporation system (Bio-Rad Laboratories Inc.). Point mutants
171 were cultured in RPMI 1640 medium containing L-glutamine.

172

173 **Hybridoma production**

174 As described in detail previously [36, 39], three 4-week-old female BALB/c mice were
175 immunized by intraperitoneal (i.p.) injection of 1×10^8 LN229/hPDPN cells together with
176 Imject Alum (Thermo Fisher Scientific Inc.) [30]. A booster injection was administered
177 i.p. 2 days before the mice were euthanized by cervical dislocation. Spleen cells were
178 harvested and fused with P3U1 cells using PEG1500 (Roche Diagnostics, Indianapolis,

179 IN, USA). The hybridomas were cultured in RPMI 1640 medium containing
180 hypoxanthine, aminopterin, and thymidine selection medium supplement (Thermo Fisher
181 Scientific Inc.). The culture supernatants were screened using an enzyme-linked
182 immunosorbent assay (ELISA) and recombinant human PDPN purified from
183 LN229/hPDPN cells [30]. Proteins (1 μg/ml) were immobilized on Nunc Maxisorp 96-
184 well immunoplates (Thermo Fisher Scientific Inc.) for 30 min. After blocking with 1%
185 bovine serum albumin (BSA) in 0.05% Tween20/phosphate-buffered saline (PBS)
186 (Nacalai Tesque, Inc.), the plates were incubated with culture supernatants, followed by
187 the addition of peroxidase-conjugated anti-mouse IgG diluted 1:2000 (Dako; Agilent
188 Technologies, Inc., Santa Clara, CA, USA). The enzymatic reaction was conducted using
189 a 1-Step Ultra TMB-ELISA (Thermo Fisher Scientific Inc.). Optical density was
190 measured at 655 nm using an iMark microplate reader (Bio-Rad Laboratories Inc.).
191
192 **Flow cytometry**
193 As described in detail previously [36, 39], cell lines were harvested after brief exposure
194 to 0.25% Trypsin/1 mM EDTA (Nacalai Tesque, Inc.). After washing with 0.1% BSA in
195 PBS, the cells were treated with primary mAbs for 30 min at 4°C, followed by treatment
196 with Oregon Green 488-conjugated to goat anti-mouse IgG or anti-rat IgG (Thermo
197 Fisher Scientific Inc.). Fluorescence data were acquired using a Cell Analyzer EC800
198 (Sony Corp., Tokyo, Japan).
199
200 **Immunohistochemical analyses**
201 As described in detail previously [36, 39], 4-μm-thick tissue sections were deparaffinized
202 using xylene and rehydrated. After antigen retrieval, (autoclaving using citrate buffer, pH

203 6.0), sections were incubated with 1 μg/ml of LpMab-21 for 1 h at room temperature, and
204 immunocomplexes were treated with an Envision+ Kit (Dako) for 30 min, color was
205 developed using 3, 3-diaminobenzidine tetrahydrochloride (DAB, Dako) for 5 min.
206 Sections were then counterstained with hematoxylin (Wako Pure Chemical Industries
207 Ltd.).
208

209 **Results**

210 **Generation of a novel anti-hPDPN mAb (LpMab-21)**

211 We first immunized one mouse with the LN229/hPDPN, and harvested spleen cells were
212 fused with P3U1. The ELISA screening was performed with supernatants from 960
213 hybridomas. Among 135 ELISA-positive wells, 19 wells reacted with LN229/hPDPN,
214 but not with LN229 in flow cytometry. We performed single cell cloning for 19 wells by
215 limiting dilution, and could obtain 14 hybridomas. Among them, we previously reported
216 five clones including LpMab-10, LpMab-12, LpMab-13, LpMab-17, and LpMab-19 [30-
217 36, 38, 39, 43]. In this study, we newly report LpMab-21 (IgG_{2a}, kappa), which was the
218 first IgG_{2a} mouse anti-hPDPN mAb in our study. Flow cytometry revealed that LpMab-
219 21 reacted with LN229/hPDPN cells but not with LN229 cells that were hPDPN-negative
220 (Fig. 1A). LpMab-21 detected endogenous hPDPN, which is expressed in the
221 glioblastoma cell line LN319, but not in LN319/hPDPN-KO cells (PDIS-6) (Fig. 1B).

222 LpMab-21 detected the expression of hPDPN in normal cells such as a
223 lymphatic endothelial cells (LECs) as well as in the mesothelial cell line Met-5A (Fig.
224 2A). The positive-control LpMab-17 reacted with LECs and Met-5A cells (Fig. 2B).
225 LpMab-21 detected endogenous hPDPN, which is expressed in the kidney epithelial cell
226 line HEK-293T, but not in HEK-293T/hPDPN-KO cells (PDIS-2) (Fig. 2C).

227 We next investigated whether LpMab-21 was suitable for
228 immunohistochemical analyses (Fig. 3). Consistent with the expression of hPDPN by
229 lymphatic endothelial cells [44], LpMab-21 reacted with lymphatic endothelial cells of
230 the esophagus (Fig. 3A), colon (Fig. 3C), lung (Fig. 3D), kidney (Fig. 3E), and rectum
231 (Fig. 3F). LpMab-21 detected hPDPN expressed by basal keratinocytes of the esophagus
232 (Fig. 3A) and myoepithelial cells of breast glands (Fig. 3B). In contrast, LpMab-21 did

233 not detect hPDPN expression in type I alveolar cells (Fig. 3D) and podocytes of the renal
234 glomerulus (Fig. 3E). These results indicate that the epitope recognized by LpMab-21 is
235 expressed by certain cell types [45].
236

237 **Flow cytometric and immunohistochemical analyses using LpMab-21 to detect**
238 **hPDPN expression in cancers**

239 PDPN is expressed by cancers such as brain tumors, mesotheliomas, oral cancers, lung
240 cancers, esophageal cancers, testicular cancers, and osteosarcoma [1, 9, 32]. Flow
241 cytometry using LpMab-21 detected endogenous expression of PDPN by the human
242 cancer cell lines as follows: mesothelioma, NCI-H226; oral squamous cell carcinoma,
243 HSC-2 and HSC-4; squamous cell carcinoma of the lung, PC-10; and human
244 osteosarcoma, U-2 OS and MG-63 (Fig. 4A). LpMab-17 detected PDPN expression by
245 all cell lines (Fig. 4B).

246 Immunohistochemical analysis (with or without antigen retrieval) using
247 LpMab-21 detected membrane-associated PDPN expression in the human tumor tissues
248 as follows: glioblastoma (Fig. 5A), oral squamous cell carcinoma (OSCC) (Fig. 5B), and
249 a seminoma (Fig. 5C). LpMab-21 reacted with lymphatic endothelial cells in OSCC
250 tissues (Fig. 5D) but not with vascular endothelial cells (Fig. 5D), demonstrating that
251 LpMab-21 is useful for detecting lymphatic endothelial cells in cancer tissues.
252

253 **Characterization of LpMab-21 using glycan-deficient cell lines**

254 Human PDPN is *O*-glycosylated, but not *N*-glycosylated [6, 24, 46-48]. In this study, we
255 generated a GnT-1-knockout (KO) cell line (CHO-S/GnT-1-KO, PDIS-9) and a CMP-
256 sialic acid transporter (SLC35A1)-knockout (KO) cell line (CHO-S/SLC35A1-KO,

257 PDIS-14) by transfecting them with TALEN and CRISPR/Cas plasmids, respectively
258 (Table 1). PDIS-9 and PDIS-14 cells were screened using leukoagglutinin from *Phaseolus*
259 *vulgaris* (L-PHA) and MAL-II, respectively. When we used the hPDPN expression vector
260 to transfect PDIS-9 and PDIS-14 cells, we found that LpMab-21 reacted with CHO-
261 S/hPDPN and PDIS-9/hPDPN cells but not with PDIS-14/hPDPN cells (Fig. 6A and B).
262 We further generated a GnT-1-knockout (KO) cell line (HEK-293T/GnT-1-KO, PDIS-1
263 or PDIS-12) and a CMP-sialic acid transporter (SLC35A1)-knockout (KO) cell line
264 (HEK-293T/SLC35A1-KO, PDIS-22) by transfecting them with TALEN and
265 CRISPR/Cas plasmids, respectively (Table 1). PDIS-1 and PDIS-12 cells were screened
266 using L-PHA. PDIS-22 cells were screened using MAL-II. We found that LpMab-21
267 reacted with HEK-293T, PDIS-1, and PDIS-12 cells but not with PDIS-22 cells
268 (Supplementary Fig. 1). These results indicate that the hPDPN epitope recognized by
269 LpMab-21 includes a peptide sequence linked to sialic acid.
270

271 **Epitope mapping of LpMab-21**

272 We expressed hPDPN deletion mutants in CHO-K1 cells (Fig. 7A). LpMab-21 detected
273 dN23, dN37, dN46, dN55, and dN64. In contrast, LpMab-21 did not react with dN75,
274 dN85, dN95, or dN105, indicating that the N-terminus of the epitope recognized by
275 LpMab-21 resides between hPDPN Thr65 and Val75 (Fig. 7B). All deletion mutants were
276 detected using the anti-MAP-tag mAb (Fig. 7C).

277 Next, we generated stable CHO-S cell lines expressing the hPDPN point
278 mutants T65A, T66A, T70A, S71A, S74A, T76A, T85A, S86A, and S88A (Fig. 8A).
279 These designations were chosen, because the epitope of LpMab-21 includes a sialylated
280 *O*-glycan (Fig. 6) and starts between residues Thr65 and Val75 (Fig. 7). LpMab-21

281 reacted with all transfectants, except for T76A (Fig. 8B). All point mutants targeting
282 Ser/Thr residues were detected by LpMab-17 (Fig. 8C). Together, these data support the
283 conclusion that the epitope recognized by LpMab-21 includes sialic acid linked to PDPN
284 Thr76.

285 We used alanine scanning to localize the epitope recognized by LpMab-21 near
286 hPDPN Thr76. Thus, nine hPDPN point mutants (Ser74–Thr85) were transiently
287 expressed in CHO-K1 cells. LpMab-21 did not detect T76A, G77A, I78A, or R79A. In
288 contrast, LpMab-12, which recognizes an epitope comprising hPDPN Thr52, detected
289 each point mutant (Fig. 9B), indicating that Thr76–Arg79 is the minimum epitope
290 recognized by LpMab-21. We summarized and compared LpMab-21 with the several
291 anti-hPDPN mAbs (Table 2).
292

293 **Discussion**

294 The anti-hPDPN mAb (NZ-1) detects hPDPN with high specificity and
295 sensitivity [6, 10, 25]. Moreover NZ-1, which is also useful for detecting the PA epitope
296 tag [49, 50], is efficiently internalized by glioma cell lines, accumulates in tumors *in vivo,*
297 and is therefore a suitable candidate for therapy for malignant gliomas [5, 10]. Further,
298 NZ-1 inhibits tumor cell-induced platelet aggregation and tumor metastasis [23]. NZ-1
299 mediates antibody-dependent cellular cytotoxicity (ADCC) and complement-dependent
300 cytotoxicity (CDC) against tumor cells that express hPDPN [51]. Moreover, NZ-1 is
301 suitable for western blotting, flow cytometry, immunohistochemistry, and
302 immunoprecipitation [51]. However, NZ-1 was produced using synthetic peptide [6];
303 therefore, further mAbs against hPDPN, especially anti-glycopeptide mAbs are necessary
304 to investigate the structure and function of PDPN.

305 Previously, we developed the original technology to produce cancer-specific
306 mAbs that detect cell type-specific posttranslational modifications of the same protein
307 [30]. We used LN229/hPDPN cells as the immunogen to elicit novel anti-PDPN mAbs.
308 We produced several clones including LpMab-2, LpMab-3, and LpMab-9 as anti-
309 glycopeptide mAbs [30]. Recently, we further immunized mice with LN229/hPDPN cells
310 to develop further anti-glycopeptide mAbs against human PDPN, and characterized
311 several clones including LpMab-12 and LpMab-19. In this study, we characterized
312 another clone LpMab-21, which detects many human cancer cell lines that express PDPN,
313 such as those derived from glioblastomas, lung squamous cell carcinomas, oral squamous
314 cell carcinomas, osteosarcomas, and malignant mesotheliomas. The isotypes of
315 previously established anti-PDPN mAbs are IgG_1 (seven clones) and IgG_3 (one clone).
316 However, the applications of mouse IgG_3 mAbs are limited because they often aggregate

317 [52]. Moreover, mouse IgG_1 and IgG_3 isotypes do not induce ADCC or CDC. Therefore,
318 we required chimeric mAbs using human IgG_1 to investigate these activities [33]. LpMab-
319 21 (IgG_{2a} subclass) could be used to investigate the function of anti-tumor activities in
320 xenograft models because LpMab-21 induced ADCC and CDC (data not shown).

321 Furthermore, we need several glycan-deficient cell lines such as sialic acid
322 deficient or *N*-glycan deficient cell lines to characterize those mAbs. In this study, we
323 successfully produced several glycan-deficient cell lines such as sialic acid deficient
324 (PDIS-14 and PDIS-22) or N-glycan deficient cell lines (PDIS-1, PDIS-9, and PDIS-12)
325 using CRISPR/Cas and TALEN systems. Using those cell lines, we determined that the
326 epitope of LpMab-21 includes sialic acids, indicating that we can also investigate whether
327 novel mAbs against the other membrane proteins possess sialic acids or N-glycans.

328 We showed here that LpMab-21 detected glioblastomas, oral cancers, and
329 seminomas (Fig. 5) as well as normal cells such as lymphatic endothelial cells, basal
330 epithelial cells of the esophagus, and myoepithelial cells of breast glands (Fig. 3). In
331 contrast, LpMab-21 did not react with the renal glomerulus or with type I alveolar cells
332 (Fig. 3), indicating that sialylation of hPDPN is tissue-specific.

333 In conclusion, LpMab-21 shows promise for investigating the expression and
334 function of hPDPN in cancers and normal tissues. Further, mAbs that recognize different
335 epitopes of hPDPN should serve as powerful tools for identifying the function of hPDPN.
336

337 **Acknowledgments**

338 We thank Noriko Saidoh and Kanae Yoshida for their excellent technical assistance. This
339 work was supported in part by the Basic Science and Platform Technology Program for
340 Innovative Biological Medicine from Japan Agency for Medical Research and

development, AMED (Y.K.), by the Platform for Drug Discovery, Informatics, and Structural Life Science (PDIS) from AMED (Y.K.), by the Practical Research for Innovative Cancer Control from AMED (Y.K.); by JSPS KAKENHI Grant Number 26440019 (M.K.K.), 25462242 (Y.K.), and 16K10748 (Y.K.), and by the Regional Innovation Strategy Support Program from the Ministry of Education, Culture, Sports, Science and Technology (MEXT) of Japan (Y.K.). This work was performed in part under the Cooperative Research Program of Institute for Protein Research, Osaka University, CR-15-05 and CR-16-05. The authors would like to thank Enago (www.enago.jp) for the English language review.

Conflict of Interest

No declared.

354 **References**

355

356 1. Martin-Villar, E., F. G. Scholl, C. Gamallo, M. M. Yurrita, M. Munoz-Guerra,
357 J. Cruces, et al. 2005. Characterization of human PA2.26 antigen (T1alpha-2, podoplanin),
358 a small membrane mucin induced in oral squamous cell carcinomas. Int J Cancer. 113:
359 899-910.

360 2. Yuan, P., S. Temam, A. El-Naggar, X. Zhou, D. Liu, J. Lee, et al. 2006.
361 Overexpression of podoplanin in oral cancer and its association with poor clinical
362 outcome. Cancer. 107: 563-9.

363 3. Takagi, S., T. Oh-hara, S. Sato, B. Gong, M. Takami, N. Fujita. 2014.
364 Expression of Aggrus/podoplanin in bladder cancer and its role in pulmonary metastasis.
365 Int J Cancer. 134: 2605-14.

366 4. Kunita, A., T. G. Kashima, A. Ohazama, A. E. Grigoriadis, M. Fukayama. 2011.
367 Podoplanin is regulated by AP-1 and promotes platelet aggregation and cell migration in
368 osteosarcoma. Am J Pathol. 179: 1041-9.

369 5. Chandramohan, V., X. Bao, M. Kato Kaneko, Y. Kato, S. T. Keir, S. E.
370 Szafranski, et al. 2013. Recombinant anti-podoplanin (NZ-1) immunotoxin for the
371 treatment of malignant brain tumors. Int J Cancer. 132: 2339-48.

372 6. Kato, Y., M. K. Kaneko, A. Kuno, N. Uchiyama, K. Amano, Y. Chiba, et al.
373 2006. Inhibition of tumor cell-induced platelet aggregation using a novel anti-podoplanin
374 antibody reacting with its platelet-aggregation-stimulating domain. Biochem Biophys
375 Res Commun. 349: 1301-7.

376 7. Mishima, K., Y. Kato, M. K. Kaneko, Y. Nakazawa, A. Kunita, N. Fujita, et al.
377 2006. Podoplanin expression in primary central nervous system germ cell tumors: a useful

378 histological marker for the diagnosis of germinoma. Acta Neuropathol (Berl). 111: 563-
379 8.
380 8. Mishima, K., Y. Kato, M. K. Kaneko, R. Nishikawa, T. Hirose, M. Matsutani.
381 2006. Increased expression of podoplanin in malignant astrocytic tumors as a novel
382 molecular marker of malignant progression. Acta Neuropathol (Berl). 111: 483-8.
383 9. Abe, S., Y. Morita, M. K. Kaneko, M. Hanibuchi, Y. Tsujimoto, H. Goto, et al.
384 2013. A novel targeting therapy of malignant mesothelioma using anti-podoplanin
385 antibody. J Immunol. 190: 6239-49.
386 10. Kato, Y., G. Vaidyanathan, M. K. Kaneko, K. Mishima, N. Srivastava, V.
387 Chandramohan, et al. 2010. Evaluation of anti-podoplanin rat monoclonal antibody NZ-
388 1 for targeting malignant gliomas. Nucl Med Biol. 37: 785-94.
389 11. Kato, Y., N. Fujita, A. Kunita, S. Sato, M. Kaneko, M. Osawa, et al. 2003.
390 Molecular identification of Aggrus/T1alpha as a platelet aggregation-inducing factor
391 expressed in colorectal tumors. J Biol Chem. 278: 51599-605.
392 12. Kato, Y., I. Sasagawa, M. Kaneko, M. Osawa, N. Fujita, T. Tsuruo. 2004.
393 Aggrus: A diagnostic marker that distinguishes seminoma from embryonal carcinoma in
394 testicular germ cell tumors. Oncogene. 23: 8552-6.
395 13. Kato, Y., M. Kaneko, M. Sata, N. Fujita, T. Tsuruo, M. Osawa. 2005. Enhanced
396 expression of Aggrus (T1alpha/podoplanin), a platelet-aggregation-inducing factor in
397 lung squamous cell carcinoma. Tumor Biol. 26: 195-200.
398 14. Pula, B., A. Jethon, A. Piotrowska, A. Gomulkiewicz, T. Owczarek, J. Calik, et
399 al. 2011. Podoplanin expression by cancer-associated fibroblasts predicts poor outcome
400 in invasive ductal breast carcinoma. Histopathology. 59: 1249-60.
401 15. Kawase, A., G. Ishii, K. Nagai, T. Ito, T. Nagano, Y. Murata, et al. 2008.

402 Podoplanin expression by cancer associated fibroblasts predicts poor prognosis of lung
403 adenocarcinoma. Int J Cancer. 123: 1053-9.
404 16. Hoshino, A., G. Ishii, T. Ito, K. Aoyagi, Y. Ohtaki, K. Nagai, et al. 2011.
405 Podoplanin-positive fibroblasts enhance lung adenocarcinoma tumor formation:
406 podoplanin in fibroblast functions for tumor progression. Cancer Res. 71: 4769-79.
407 17. Schoppmann, S. F., B. Jesch, M. F. Riegler, F. Maroske, K. Schwameis, G.
408 Jomrich, et al. 2013. Podoplanin expressing cancer associated fibroblasts are associated
409 with unfavourable prognosis in adenocarcinoma of the esophagus. Clin Exp Metastasis.
410 30: 441-6.
411 18. Shindo, K., S. Aishima, K. Ohuchida, K. Fujiwara, M. Fujino, Y. Mizuuchi, et
412 al. 2013. Podoplanin expression in cancer-associated fibroblasts enhances tumor
413 progression of invasive ductal carcinoma of the pancreas. Mol Cancer. 12: 168.
414 19. Inoue, H., H. Tsuchiya, Y. Miyazaki, K. Kikuchi, F. Ide, H. Sakashita, et al.
415 2014. Podoplanin expressing cancer-associated fibroblasts in oral cancer. Tumour Biol.
416 35: 11345-52.
417 20. Kunita, A., T. G. Kashima, Y. Morishita, M. Fukayama, Y. Kato, T. Tsuruo, et
418 al. 2007. The platelet aggregation-inducing factor aggrus/podoplanin promotes
419 pulmonary metastasis. Am J Pathol. 170: 1337-47.
420 21. Kaneko, M. K., Y. Kato, T. Kitano, M. Osawa. 2006. Conservation of a platelet
421 activating domain of Aggrus/podoplanin as a platelet aggregation-inducing factor. Gene.
422 378: 52-7.
423 22. Suzuki-Inoue, K., Y. Kato, O. Inoue, M. K. Kaneko, K. Mishima, Y. Yatomi, et
424 al. 2007. Involvement of the snake toxin receptor CLEC-2, in podoplanin-mediated
425 platelet activation, by cancer cells. J Biol Chem. 282: 25993-6001.

426 23. Kato, Y., M. K. Kaneko, A. Kunita, H. Ito, A. Kameyama, S. Ogasawara, et al.
427 2008. Molecular analysis of the pathophysiological binding of the platelet aggregation-
428 inducing factor podoplanin to the C-type lectin-like receptor CLEC-2. Cancer Sci. 99: 54-
429 61.
430 24. Nagae, M., K. Morita-Matsumoto, M. Kato, M. K. Kaneko, Y. Kato, Y.
431 Yamaguchi. 2014. A Platform of C-Type lectin-like receptor CLEC-2 for binding O-
432 glycosylated podoplanin and nonglycosylated rhodocytin. Structure. 22: 1711-21.
433 25. Ogasawara, S., M. K. Kaneko, J. E. Price, Y. Kato. 2008. Characterization of
434 anti-podoplanin monoclonal antibodies: critical epitopes for neutralizing the interaction
435 between podoplanin and CLEC-2. Hybridoma. 27: 259-67.
436 26. Takagi, S., S. Sato, T. Oh-hara, M. Takami, S. Koike, Y. Mishima, et al. 2013.
437 Platelets promote tumor growth and metastasis via direct interaction between
438 Aggrus/podoplanin and CLEC-2. PLoS One. 8: e73609.
439 27. Nakazawa, Y., S. Takagi, S. Sato, T. Oh-hara, S. Koike, M. Takami, et al. 2011.
440 Prevention of hematogenous metastasis by neutralizing mice and its chimeric anti-
441 Aggrus/podoplanin antibodies. Cancer Sci. 102: 2051-7.
442 28. Marks, A., D. R. Sutherland, D. Bailey, J. Iglesias, J. Law, M. Lei, et al. 1999.
443 Characterization and distribution of an oncofetal antigen (M2A antigen) expressed on
444 testicular germ cell tumours. Br J Cancer. 80: 569-78.
445 29. Kono, T., M. Shimoda, M. Takahashi, K. Matsumoto, T. Yoshimoto, M.
446 Mizutani, et al. 2007. Immunohistochemical detection of the lymphatic marker
447 podoplanin in diverse types of human cancer cells using a novel antibody. Int J Oncol.
448 31: 501-8.
449 30. Kato, Y., M. K. Kaneko. 2014. A cancer-specific monoclonal antibody

450 recognizes the aberrantly glycosylated podoplanin. Sci Rep. 4: 5924.

451 31. Kaneko, M. K., H. Oki, Y. Hozumi, X. Liu, S. Ogasawara, M. Takagi, et al.
452 2015. Monoclonal antibody LpMab-9 recognizes O-glycosylated N-terminus of human
453 podoplanin. Monoclon Antib Immunodiagn Immunother. 34: 310-7.

454 32. Kaneko, M. K., H. Oki, S. Ogasawara, M. Takagi, Y. Kato. 2015. Anti-
455 podoplanin monoclonal antibody LpMab-7 detects metastatic legions of osteosarcoma.
456 Monoclon Antib Immunodiagn Immunother. 34: 154-61.

457 33. Kato, Y., A. Kunita, S. Abe, S. Ogasawara, Y. Fujii, H. Oki, et al. 2015. The
458 chimeric antibody chLpMab-7 targeting human podoplanin suppresses pulmonary
459 metastasis via ADCC and CDC rather than via its neutralizing activity. Oncotarget. 6:
460 36003-18.

461 34. Ogasawara, S., H. Oki, M. K. Kaneko, Y. Hozumi, X. Liu, R. Honma, et al.
462 2015. Development of monoclonal antibody LpMab-10 recognizing non-glycosylated
463 PLAG1/2 domain including Thr34 of human podoplanin. Monoclon Antib Immunodiagn
464 Immunother. 34: 318-26.

465 35. Oki, H., M. K. Kaneko, S. Ogasawara, Y. Tsujimoto, X. Liu, M. Sugawara, et
466 al. 2015. Characterization of a monoclonal antibody LpMab-7 recognizing non-PLAG
467 domain of podoplanin. Monoclon Antib Immunodiagn Immunother. 34: 174-80.

468 36. Oki, H., S. Ogasawara, M. K. Kaneko, M. Takagi, M. Yamauchi, Y. Kato. 2015.
469 Characterization of monoclonal antibody LpMab-3 recognizing sialylated glycopeptide
470 of podoplanin. Monoclon Antib Immunodiagn Immunother. 34: 44-50.

471 37. Kato, Y., S. Ogasawara, H. Oki, P. Goichberg, R. Honma, Y. Fujii, et al. 2016.
472 LpMab-12 Established by CasMab Technology Specifically Detects Sialylated O-Glycan
473 on Thr52 of Platelet Aggregation-Stimulating Domain of Human Podoplanin. PLoS One.

474 11: e0152912.

475 38. Kato, Y., S. Ogasawara, H. Oki, R. Honma, M. Takagi, Y. Fujii, et al. 2016.
476 Novel monoclonal antibody LpMab-17 developed by CasMab technology distinguishes
477 human podoplanin from monkey podoplanin. Monoclon Antib Immunodiagn
478 Immunother. 35: 109-16.

479 39. Ogasawara, S., M. K. Kaneko, R. Honma, H. Oki, Y. Fujii, M. Takagi, et al.
480 2016. Establishment of Mouse Monoclonal Antibody LpMab-13 against Human
481 Podoplanin Monoclon Antib Immunodiagn Immunother. DOI:
482 10.1089/mab.2016.0006.rev.

483 40. Hayatsu, N., S. Ogasawara, M. K. Kaneko, Y. Kato, H. Narimatsu. 2008.
484 Expression of highly sulfated keratan sulfate synthesized in human glioblastoma cells.
485 Biochem Biophys Res Commun. 368: 217-22.

486 41. Kaji, C., Y. Tsujimoto, M. Kato Kaneko, Y. Kato, Y. Sawa. 2012.
487 Immunohistochemical Examination of Novel Rat Monoclonal Antibodies against Mouse
488 and Human Podoplanin. Acta Histochem Cytochem. 45: 227-37.

489 42. Honma, R., S. Ogasawara, M. Kaneko, Y. Fujii, H. Oki, T. Nakamura, et al.
490 2016. PMab-44 Detects Bovine Podoplanin in Immunohistochemistry. Monoclon Antib
491 Immunodiagn Immunother. DOI: 10.1089/mab.2016.0016.

492 43. Ogasawara, S., M. K. Kaneko, Y. Kato. 2016. LpMab-19 Recognizes Sialylated
493 O-Glycan on Thr76 of Human Podoplanin. Monoclonal antibodies in immunodiagnosis
494 and immunotherapy.

495 44. Breiteneder-Geleff, S., A. Soleiman, H. Kowalski, R. Horvat, G. Amann, E.
496 Kriehuber, et al. 1999. Angiosarcomas express mixed endothelial phenotypes of blood
497 and lymphatic capillaries: podoplanin as a specific marker for lymphatic endothelium.

498 Am J Pathol. 154: 385-94.

499 45. Schacht, V., S. S. Dadras, L. A. Johnson, D. G. Jackson, Y. K. Hong, M. Detmar.
500 2005. Up-regulation of the lymphatic marker podoplanin, a mucin-type transmembrane
501 glycoprotein, in human squamous cell carcinomas and germ cell tumors. Am J Pathol.
502 166: 913-21.

503 46. Kaneko, M., Y. Kato, A. Kunita, N. Fujita, T. Tsuruo, M. Osawa. 2004.
504 Functional sialylated O-glycan to platelet aggregation on Aggrus (T1alpha/podoplanin)
505 molecules expressed in Chinese Hamster Ovary cells. J Biol Chem. 279: 38838-43.

506 47. Kaneko, M. K., Y. Kato, A. Kameyama, H. Ito, A. Kuno, J. Hirabayashi, et al.
507 2007. Functional glycosylation of human podoplanin: glycan structure of platelet
508 aggregation-inducing factor. FEBS Lett. 581: 331-6.

509 48. Kuno, A., Y. Kato, A. Matsuda, M. K. Kaneko, H. Ito, K. Amano, et al. 2009.
510 Focused differential glycan analysis with the platform antibody-assisted lectin profiling
511 for glycan-related biomarker verification. Mol Cell Proteomics. 8: 99-108.

512 49. Fujii, Y., M. Kaneko, M. Neyazaki, T. Nogi, Y. Kato, J. Takagi. 2014. PA tag: a
513 versatile protein tagging system using a super high affinity antibody against a
514 dodecapeptide derived from human podoplanin. Protein Expr Purif. 95: 240-7.

515 50. Fujii, Y., Y. Matsunaga, T. Arimori, Y. Kitago, S. Ogasawara, M. K. Kaneko, et
516 al. 2016. Tailored placement of a turn-forming PA tag into the structured domain of a
517 protein to probe its conformational state. J Cell Sci. 129: 1512-22.

518 51. Kaneko, M. K., A. Kunita, S. Abe, Y. Tsujimoto, M. Fukayama, K. Goto, et al.
519 2012. Chimeric anti-podoplanin antibody suppresses tumor metastasis through
520 neutralization and antibody-dependent cellular cytotoxicity. Cancer Sci. 103: 1913-9.

521 52. Abdelmoula, M., F. Spertini, T. Shibata, Y. Gyotoku, S. Luzuy, P. H. Lambert,

522 et al. 1989. IgG3 is the major source of cryoglobulins in mice. J Immunol. 143: 526-32.

523

524

525 **Figure legends**

526 **Figure 1. Flow cytometric analysis using LpMab-21 to detect hPDPN expression**. (A)
527 LN229 and LN229/hPDPN cells were treated with LpMab-21 (1 μg/ml, red) or PBS
528 (black) for 30 min at 4°C followed by treatment with anti-mouse IgG-Oregon green. (B)
529 LN319 and LN319/hPDPN-KO cells (PDIS-6) were treated with LpMab-21 (1 μg/ml,
530 red) or PBS (black) for 30 min at 4°C followed by addition of anti-mouse IgG-Oregon
531 green. Fluorescence data were collected using a Cell Analyzer EC800. Geometric Mean
532 was described.

533

534 **Figure 2. Flow cytometric analysis using LpMab-21 to detect hPDPN expression in**
535 **normal cells.** (A) Human lymphatic endothelial cells (LECs) and human mesothelial cells
536 (Met-5A) were reacted with LpMab-21 (1 μg/ml, red) or PBS (black) for 30 min at 4°C,
537 followed by treatment with anti-mouse IgG-Oregon green. (B) LEC and Met-5A cells
538 were treated with LpMab-17 (1 μg/ml, red) or PBS (black) for 30 min at 4°C, followed
539 by treatment with anti-mouse IgG-Oregon green. (C) The human embryonic renal
540 epithelial cell line (HEK-293T) and HEK-293T/hPDPN-KO cells (PDIS-2) were reacted
541 with LpMab-21 (1 μg/ml, red) or PBS (black) for 30 min at 4°C, followed by addition of
542 anti-mouse IgG-Oregon green. Fluorescence data were acquired using a Cell Analyzer
543 EC800. Geometric Mean was described.

544

545 **Figure 3. Immunohistochemical analysis using LpMab-21 to detect PDPN**
546 **expression in normal human tissues.** Tissues harvested from the esophagus (A), breast
547 (B), colon (C), lung (D), kidney (E), and rectum (F). After antigen retrieval procedure,
548 sections were incubated with 1 μg/ml of LpMab-21, reacted with the Envision+ kit, color

549 was developed using DAB, and samples were then counterstained with hematoxylin.
550 Arrowheads: lymphatic endothelial cells. Scale bar = 100 μm.
551
552 **Figure 4. Flow cytometric analysis using LpMab-21 to detect PDPN expression in**
553 **human cancer cells**. Human cell lines analyzed were as follows: mesothelioma, NCI-
554 H226; oral squamous cell carcinomas, HSC-2 and HSC-4; lung squamous cell carcinoma,
555 PC-10; and osteosarcomas U-2 OS and MG-63. Cells were treated reacted with LpMab-
556 21 (A, 1 μg/ml; red), LpMab-17 (B, 1 μg/ml; red), or PBS (A and B, black) for 30 min at
557 4°C, followed by treatment with anti-mouse IgG-Oregon green. Fluorescence data were
558 acquired using a Cell Analyzer EC800. Geometric Mean was described.
559
560 **Figure 5. Immunohistochemical analysis using LpMab-21 to detect PDPN**
561 **expression in human cancer tissues.** Tissue sections were prepared from the human
562 cancer tissues as follows: glioblastoma (GBM, A and E); oral squamous cell carcinoma
563 (OSCC; B, D, F, and H); seminoma (SE, C and G). Sections were incubated (antigen
564 retrieval omitted) with 1 μg/ml of LpMab-21 (A-D), reacted with the Envision+ kit, color
565 was developed using DAB, and samples were then counterstained with hematoxylin.
566 Sections were stained with hematoxylin and eosin as well (E-H). Arrowheads: lymphatic
567 endothelial cells. Scale bar = 100 μm.
568
569 **Figure 6. Flow cytometric analysis using LpMab-21 to detect hPDPN expression in**
570 **sialic acid-deficient cells.** CHO-S, CHO-S/hPDPN, PDIS-9/hPDPN, and PDIS-
571 14/hPDPN cells were reacted with LpMab-21 (A, 1 μg/ml; red), LpMab-21 (B, 10 μg/ml;
572 red), or LpMab-17 (C, 1 μg/ml; red), or PBS (A, B, and C; black) for 30 min at 4°C,

573 followed by treatment with anti-mouse IgG-Oregon green. Fluorescence data were
574 acquired using a Cell Analyzer EC800. Geometric Mean was described.
575
576 **Figure 7. Epitope mapping of LpMab-21 using deletion mutants of hPDPN**.
577 (A)Structures of hPDPN deletion dN23, dN37, dN46, dN55, dN64, dN75, dN85, dN95,
578 dN105. (B, C) Each hPDPN deletion mutant was reacted with LpMab-21 (B, 1 μg/ml;
579 red), PMab-1 (C, 1 μg/ml; red), or PBS (B and C, black) for 30 min at 4°C, followed by
580 treatment with anti-mouse IgG-Oregon green (B) or anti-rat IgG-Oregon green (C).
581 Fluorescence data were acquired using a Cell Analyzer EC800. Geometric Mean was
582 described.
583
584 **Figure 8.** Epitope mapping of LpMab-21 using hPDPN-Ser/Thr point mutants. (A)
585 Amino acid sequence of hPDPN encompassing Thr76. (B, C) Stable CHO-S transfectants
586 expressing hPDPN point mutants T65A, T66A, T70A, S71A, S74A, T76A, T85A, S86A,
587 and S88A were reacted with LpMab-21 (B, 1 μg/ml; red), LpMab-17 (C, 1 μg/ml; red),
588 or PBS (B and C; black) for 30 min at 4°C, followed by treatment with anti-mouse IgG-
589 Oregon green. Fluorescence data were acquired using a Cell Analyzer EC800. Geometric
590 Mean was described.
591
592 **Figure 9.** Epitope mapping of LpMab-21 using point mutants of hPDPN. Nine hPDPN
593 point Ser74–Thr85 point mutants were transiently expressed in CHO-K1 cells. Cells were
594 reacted with LpMab-21 (A, 1 μg/ml; red), LpMab-12 (B, 1 μg/ml; red), or control PBS
595 (A and B, black) for 30 min at 4°C, followed by treatment with anti-mouse IgG-Oregon
596 green. Fluorescence data were acquired using a Cell Analyzer EC800. (C) Illustration of

597 the epitope recognized by anti-hPDPN mAbs. Geometric Mean was described.

598

Table 1 Characterization of glycan-deficient or PDPN-knock out cells

Cell name	Parental cells	Targeted genes	Genom editing	Deficient
PDIS-1	HEK-293T	hsMgat1/GnT-1	TALEN	*N*-glycan
PDIS-2	HEK-293T	PDPN	CRISPR/Cas9	PDPN
PDIS-6	LN319	PDPN	CRISPR/Cas9	PDPN
PDIS-9	CHO-S	hsMgat1/GnT-1	TALEN	*N*-glycan
PDIS-12	HEK-293T	hsMgat1/GnT-1	TALEN	*N*-glycan
PDIS-14	CHO-S	SLC35A1	CRISPR/Cas9	sialic acid
PDIS-22	HEK-293T	SLC35A1	CRISPR/Cas9	sialic acid

599

600

Table 2 Characterization of anti-PDPN glycopeptide mAbs

Anti-glycopeptide mAb	subclass	Epitope		CasMab/non-CasMab	IHC (LEC, T1a, POD)
		O-glycan	pepitde		
LpMab-21	IgG2a, kappa	Thr76	Thr76–Arg79	non-CasMab	positive for only LEC
LpMab-2	IgG1, kappa	Thr55/Ser56	Thr55–Leu64	CasMab	negative
LpMab-3	IgG1, kappa	Thr76	Thr76–Glu81	non-CasMab	positive for LEC, T1a, POD
LpMab-9	IgG1, kappa	Thr25	Thr25–Asp30	non-CasMab	not applicable
LpMab-12	IgG1, kappa	Thr52	Asp49–Pro53	non-CasMab	positive for LEC, T1a, POD
LpMab-19	IgG2b, kappa	Thr76	Thr76–Arg79	non-CasMab	positive for LEC, T1a, POD

601 IHC, immunohistochemical analysis; LEC, lymphatic endothelial cells; T1a, type I alveolar cells; POD, podocyte

602

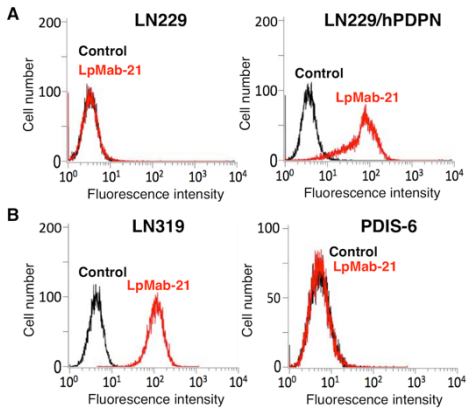

603 **Kaneko et al., Figure 1**

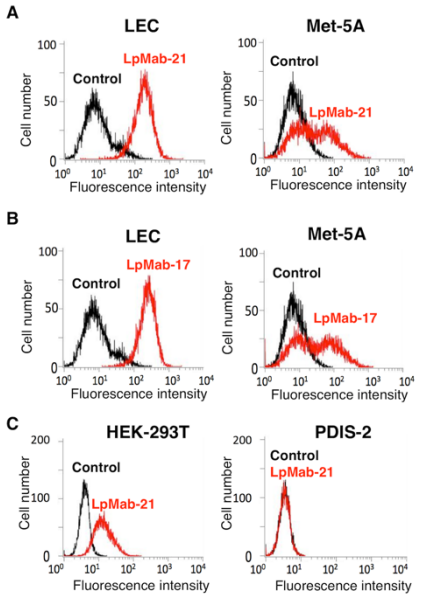

604 **Kaneko et al., Figure 2**

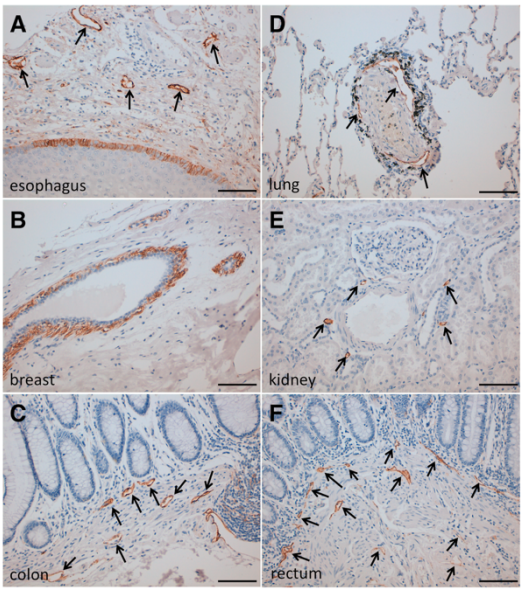

605 **Kaneko et al., Figure 3**

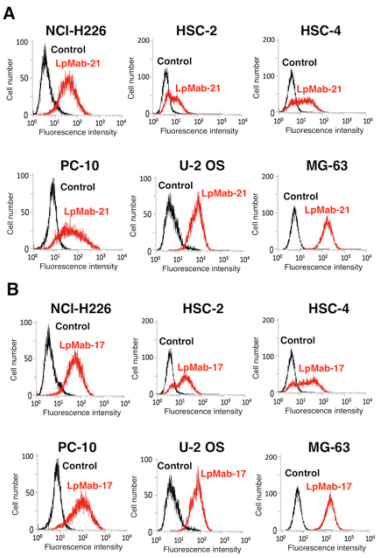

606 **Kaneko et al., Figure 4**

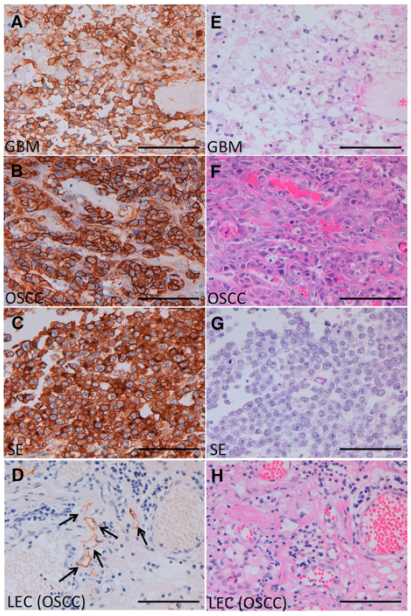

607 **Kaneko et al., Figure 5**

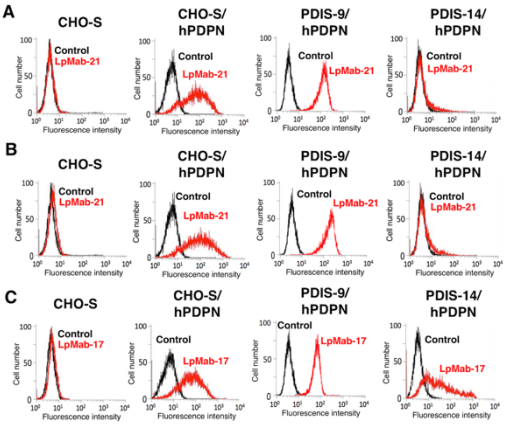

608 **Kaneko et al., Figure 6**

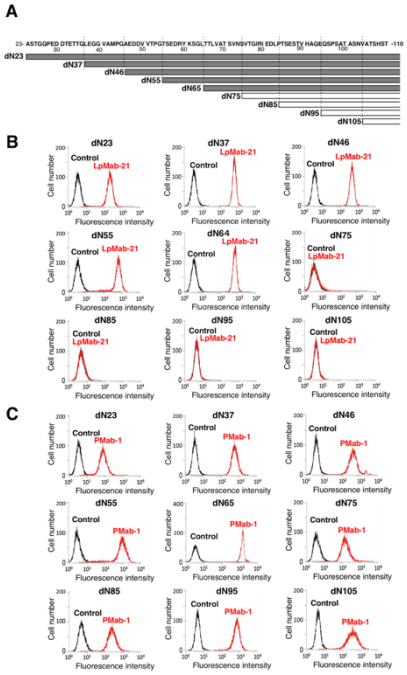

609 **Kaneko et al., Figure 7**

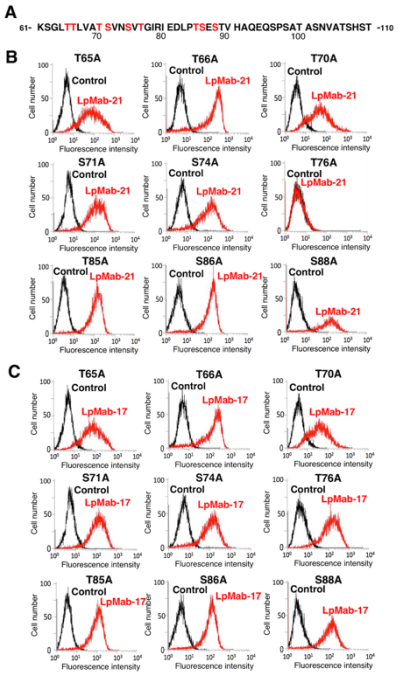

610 **Kaneko et al., Figure 8**

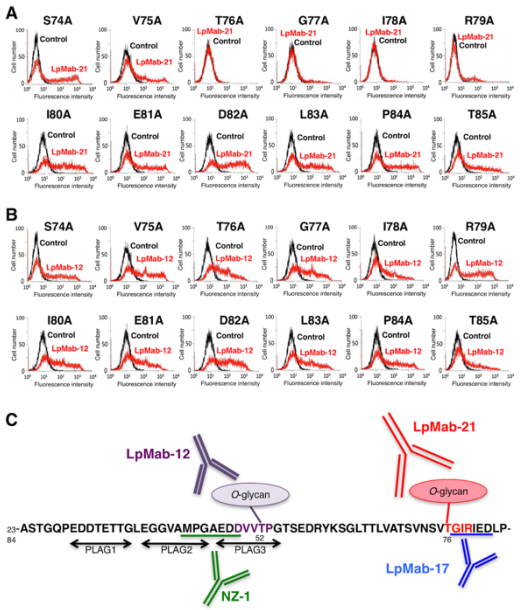

611 **Kaneko et al., Figure 9**

612